

Electrically Induced Multiple Metal-Insulator Transitions in Oxide Nanodevices

Javier del Valle,^{1,2} Yoav Kalcheim,^{1,2} Juan Trastoy,^{1,2} Aliaksei Charnukha,^{1,2} Dimitri N. Basov,^{1,2,3} and Ivan K. Schuller^{1,2}

¹*Department of Physics, University of California San Diego, La Jolla, California 92093, USA*

²*Center for Advanced Nanoscience, University of California San Diego, La Jolla, California 92093, USA*

³*Department of Physics, Columbia University, New York, New York 10027, USA*

(Received 15 June 2017; revised manuscript received 28 September 2017; published 21 November 2017)

We show that electrical resistive switching can trigger the appearance of multiple metal-insulator transitions (MITs) in VO₂ and V₂O₃ planar nanodevices. We have fabricated planar devices to electrically induce oxygen vacancy drift and filament formation. We show that oxygen migration can create ordered vanadium-oxide phases of varying stoichiometry with an intrinsic MIT, resulting in well-defined hysteresis loops in the R vs T characteristics of the device. We also show that oxygen migration induces oxide phases displaying correlated behaviors. Our results open up the possibility to electrically control the MIT, enabling alternative functionalities in memristive devices and allowing for alternative paradigms in neuromorphic computing or memory applications.

DOI: 10.1103/PhysRevApplied.8.054041

I. INTRODUCTION

Resistive switching in transition metal oxides has attracted much attention over the past decade [1–6]. Understanding the fundamental mechanisms that control this phenomenon has become a topic of increased interest with the rise of emerging technologies such as memristive memories or neuromorphic computing [7–10]. The formation of conductive filaments within the insulating oxide has been widely reported to be the origin of this resistance change in most cases [6,8,11,12], although other effects, such as changes in the interfaces, might play an important role. Depending on the mechanism that triggers the appearance of these filaments, resistive switching in metal oxides can be broadly divided into electrochemical and thermal switching [8]. Electrochemical switching by strong electric fields is induced by the drift and/or accumulation of oxygen vacancies locally changing the oxidation state [6,8]. On the other hand, thermal switching is caused by local Joule heating along the current path, which changes the resistivity [8]. Thermally assisted resistive switching is commonly observed in many correlated oxides such as VO₂ or NbO₂ which exhibit a metal-insulator transition (MIT) [13–16]. In this paper, we address the possibility to use resistive switching to generate correlated oxides within the filament and the potential functionalities it could bring about.

In this paper we show that electroforming in vanadium-oxide nanodevices triggers the appearance of multiple MITs in the system. We show that oxygen migration under strong electric fields can create ordered vanadium-oxide phases with well-defined MIT. We show that this can be accomplished at temperatures far from the MIT which allows the application of large electric fields. Our work demonstrates that systems with multiple, stable correlated phases provide a unique opportunity for observing new physics in oxide nanodevices.

In particular, the VO_x family exhibits a large number of stable, closely spaced stoichiometric phases, including the Magnéli series (V_nO_{2n-1}) [17]. Most of them are known to be strongly correlated oxides, showing a MIT in which the resistivity changes by several orders of magnitude [18]. The temperature at which the MIT takes place follows no systematic dependence with the oxygen content and very small changes on its concentration shifts the MIT by several tens of kelvin. These particular characteristics of the vanadate family make it the perfect system to use electroforming as a mean to control the properties of the MIT just by applying a voltage.

We use VO₂ and V₂O₃ planar nanodevices to explore the possibility of electroforming in two well-known oxides which exhibit a MIT, and whose electronic properties have drawn much attention in recent years [19–24]. We show that the application of a high voltage triggers the appearance of multiple MITs which manifest themselves as several resistance jumps as a function of the temperature. Most of these jumps tend to appear around well-defined transition temperatures of the vanadate family. This indicates that oxygen vacancy migration has generated crystalline oxide phases within the device and reveals that electroforming in correlated materials exhibits complex electrical behavior and rather unique functionalities to common oxides.

II. EXPERIMENT

We have grown 100-nm-thick VO₂ and V₂O₃ films on r -cut sapphire substrates using rf magnetron sputtering from a V₂O₃ target. In the case of V₂O₃ the growth is done in an 8-mTorr high-purity argon (>99.999%) atmosphere, while for the VO₂ we used a 4-mTorr argon-oxygen mixture (8% O₂). The substrate temperature during

deposition is 720 and 520 °C, respectively, and the samples are cooled at a rate of 80 °C/min (V_2O_3) and 12 °C/min (VO_2) after growth, in the same gas mixture used during the sputtering. Single-phase growth in both cases is confirmed by x-ray diffraction, epitaxially along the $\langle 012 \rangle$ direction for V_2O_3 and textured along $\langle 100 \rangle$ for VO_2 . Transport measurements show a MIT transition of over 5 orders of magnitude at 160 K for V_2O_3 and around 4 orders of magnitude at 340 K for VO_2 , evidence that for both cases high-quality films are obtained. In order to apply high electric fields in the samples, we use a planar electrode geometry with a very narrow (80–200 nm) gap [see inset in Fig. 1(a)]. The two closely spaced Ti/Au (20/40 nm thickness) electrodes are fabricated using *e*-beam lithography and *e*-beam evaporation. Optical lithography and reactive ion etching (Ar + Cl_2 plasma) are used to etch all the vanadium oxide except in the nanogap area. Using optical lithography and *e*-beam evaporation, the

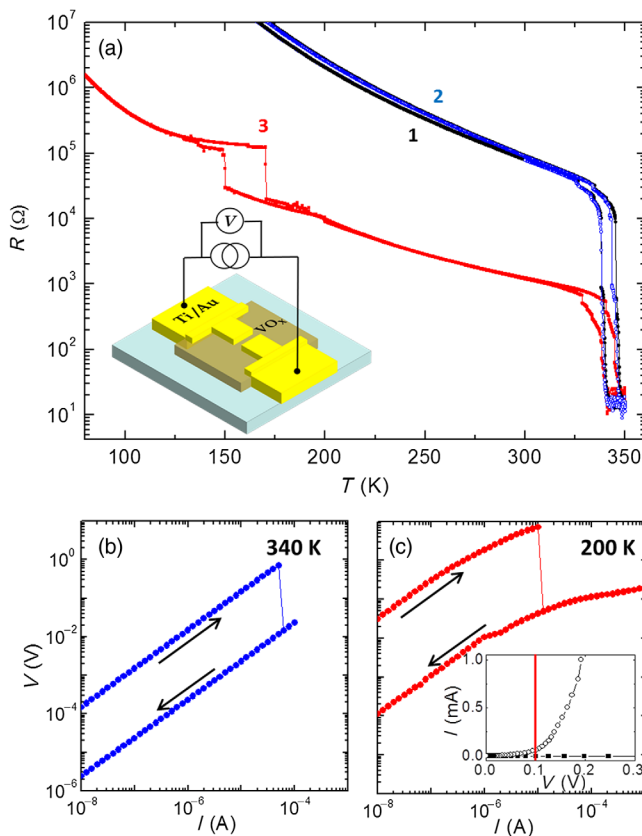


FIG. 1. (a) R vs T for the VO_2 nanodevice, measured with a 10-nA current: virgin (curve 1, black dots), after thermal switching at 340 K (curve 2, empty blue dots) and after electroforming at $T = 200$ K (curve 3, red squares). Inset: Schematic representation of the nanodevices. The VO_x films are grown on top of *r*-cut sapphire substrates (blue). (b) V vs I in a VO_2 nanodevice at $T = 340$ K. (c) V vs I in a VO_2 nanodevice at $T = 200$ K. The inset shows the same curve in a linear scale, with the high resistance state in solid squares and the low resistance state in open circles.

nanoelectrodes are extended into contact pads. Measurements are carried out on a Lakeshore TTPX cryogenic probe station, using a Keithley 6221 current source and a Keithley 2182A nanovoltmeter.

Curve 1 in Fig. 1(a) shows the resistance R as a function of temperature T for one of the VO_2 devices (~ 100 nm gap), with a MIT at 345 K, measured with a 10-nA current to avoid heating. Figure 1(b) shows the voltage V as a function of current I for the same device at a temperature of 340 K, just below the transition. As the current is ramped up, the voltage increases until there is a sudden drop in resistance of almost 2 orders of magnitude at around 1 V. This resistive switching persists as the current is ramped back down, indicating that a conductive path has been formed between the Ti/Au electrodes. After warming the sample above the MIT, the $R(T)$ curve marked as 2 in Fig. 1(a) is remeasured using a low current. Curves 1 and 2 are almost identical: i.e., neither the resistance nor the MIT have changed as a result of performing this switching. This implies that although a filament is formed in the gap while ramping the current, the change is not permanent since it can be erased by a temperature cycling.

However, a completely different behavior is observed if the same procedure is performed at lower temperatures. Figure 1(c) shows the $V(I)$ curve for the same VO_2 device at a temperature of 200 K, at which the resistance is initially above 2 M Ω . Again, a resistance drop over 2 orders of magnitude is observed, but this time at a voltage of 10 V. Immediately after this process the $R(T)$ curve 3 in Fig. 1(a) is measured. Stark differences with curves 1 and 2 are found: the resistance does not recover its preswitching value by cycling the temperature, indicating that permanent resistive switching has been achieved. Interestingly, in addition to the usual MIT of VO_2 around 345 K, a second abrupt hysteretic transition around 150 K appears.

We perform similar measurements in 20 different nanogaps, in order to obtain a statistical distribution of the temperatures at which these MITs take place. Figure 2(a) shows a histogram of the number of resistance jumps as a function of temperature for cooling (top panel) and warming (bottom panel). The jumps concentrate around two different temperatures: 130 K while reducing the temperature, and 182 K while increasing it. The transition is centered around 151 K, close to the V_2O_3 MIT, suggesting that V_2O_3 crystallites have formed within the gap. The hysteresis between warming and cooling is larger than the usually found width (~ 10 K) in V_2O_3 . Such broadening of the hysteresis has been linked to a reduction in the system size [25], indicating that these jumps are a result of small volumes of the sample undergoing a MIT.

Similar experiments in the V_2O_3 nanogaps produce analogous results: several MIT appear as a consequence of the filament formation (see Supplemental Material [26] for the V_2O_3 case). Figure 2(b) shows the jump frequency as a function of the temperature for the V_2O_3 nanogaps.

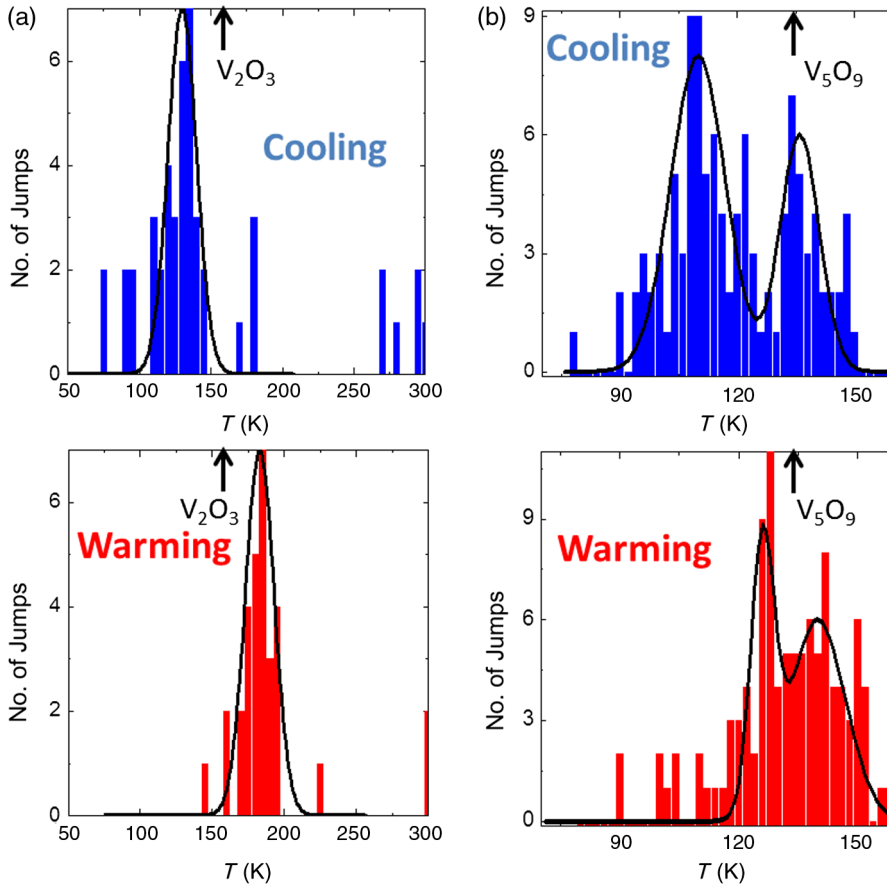


FIG. 2. Histogram of the number of jumps observed after filament electro-forming as a function of the temperature at which they appear, for cooling (blue) and heating (red), for VO_2 (a) and V_2O_3 (b) devices. Arrows mark MIT temperatures for different bulk vanadates.

The transitions concentrate around two different temperatures, both for cooling and heating, indicating that more than one VO_x phase is created within the gap. The two Gaussian distributions are approximately centered around 126 and 140 K, the latter being close to the MIT of V_5O_9 (135 K). Interestingly, since V_5O_9 has higher oxygen content than V_2O_3 , this implies that the oxidation state has been increased in some regions of the gap. However, we have not been able to identify any vanadate with a MIT close to 126 K and this transition might be coming from an off-stoichiometry or strained VO_x phase. This statistical analysis of cumulative events is widely used to obtain information in nanoscale systems subjected to great variability, such as resistive switching [27] or molecular tunnel junctions [28]; and in our case it provides indicative information about the possible phases which could be present in the gap. In order to confirm the presence of a particular phase a structural analysis would be required, which given the small size of the filaments would be extremely challenging and beyond the scope of this paper.

The role of oxygen stoichiometry can be further investigated by annealing the samples above room temperature. Figure 3(a) shows the $R(T)$ of a VO_2 device immediately after switching (curve 1), and after annealing in vacuum for 1 h at 300 K (curve 2), 350 K (curve 3), and 400 K (curve 4). The $R(T)$ changes dramatically as a result of the annealing. The resistance increases as a function of

the annealing temperature, almost recovering the full resistance and MIT of the unswitched state in the case of VO_2 (curve 4). This evolution with annealing temperature is a consequence of the oxygen vacancies redistribution during the annealing, which gradually restores the oxygen content within the gap. This reoxidation effect leaves a direct fingerprint in the transport properties: the electrically induced MIT shifts from 150 K (marked with an arrow in curve 1), corresponding to V_2O_3 , to around 175 K (marked in curve 2), closer to the MIT of the oxygen-rich V_6O_{11} . The results for the V_2O_3 devices are qualitatively similar, as shown in Fig. 3(b).

III. DISCUSSION

All these results can be understood considering two different mechanisms that can induce resistive switching: thermal phase switching and oxygen migration. At 340 K [Fig. 1(b)], thermally induced transient switching occurs [curve 2 in Fig. 1(a)]. This behavior, observed before both in VO_2 and V_2O_3 has a well-understood origin. Joule heating increases the local temperature above the MIT, parts of the gap turn metallic and the resistance drops suddenly [13–16]. Using a simple heat-transfer model (see Ref. [29]), we estimate that for the current and voltage values at which the breakdown takes place in Fig. 1(b) the temperature in the gap has risen from 340 to 344 K, enough

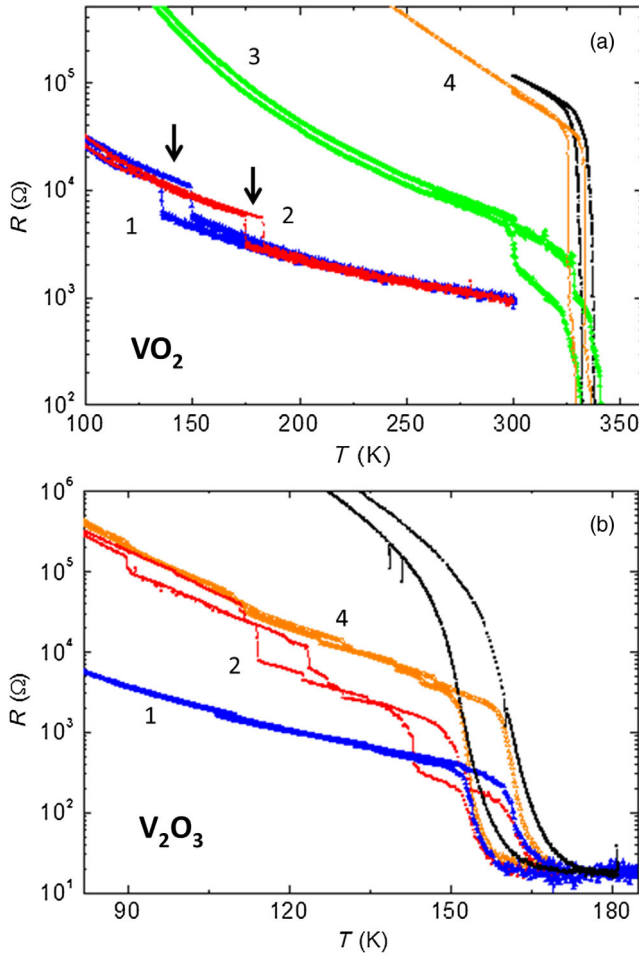


FIG. 3. R vs T for a VO_2 (a) and V_2O_3 (b) device: immediately after the resistive switching (curve 1, blue triangles); after annealing for an hour at 300 K (curve 2, red squares); at 350 K (curve 3, green diamonds); and at 400 K (curve 4, orange open circles). Virgin curves are also plotted (black open squares).

to trigger the MIT in the device. This thermal breakdown limits the power, and hence the voltage that can be applied to about 1 V in the case of Fig. 1(b). Although Joule heating seems to properly explain the origin of this breakdown, we should not overlook that the electric field might also destabilize the insulating phase and contribute to triggering the MIT [30,31].

On the other hand, at 200 K the increased resistance in the gap allows for the application of considerably higher voltages before the MIT takes place. In this case, the resistive switching occurs at an applied voltage of 10 V. The MIT at 150 K [curve 3 of Fig. 1(a)] proves that a conductive filament with its own MIT, is formed within the VO_2 matrix. In this case, the electric field is high enough to produce electromigration of oxygen vacancies, reducing the VO_2 along the filament to form different VO_x crystallites, with a different MIT. These oxygen vacancies might originate at the interface between the VO_2 and the electrodes, where the Ti layer reduces the VO_2 , creating a

vacancy reservoir, as observed for TiO_2 [8]. Once the electric field is turned on, the potential gradient will push them towards the opposite electrode, creating a filament of different stoichiometry. This process is known to take place in very short time scales (down to ~ 10 ns), having an exponential dependence as a function of the applied voltage [32]. Although the formation of reduced VO_x oxides under strong fields had previously been reported [33], they are shown here to display correlated behavior similar to existing crystalline phases. The typical resistivity of $10^{-5} \Omega\text{m}$ for the metallic phases of the VO_x family implies that the resistance values after switching are consistent with the formation of a conductive filament with a radius around 5–15 nm. This is close to filament sizes reported for other metal oxides [6,11,12].

The fact that the filament-formation mechanisms are starkly different at 340 and 200 K can be understood by analyzing the power dissipated in the gap during resistive switching. Since the dissipation is proportional to V^2/R , as the temperature is decreased the voltage expected to thermally switch the device increases. This is particularly important for materials which exhibit a MIT, as the dependence of R on T is very strong. On the other hand, electroforming mechanisms are expected to be weakly temperature dependent so the voltage at which they take place remains almost constant [7]: in our case it is around 10 V, corresponding to a field of 10^8 V/m, close to that reported by many groups [3–6,11]. These two different temperature dependences naturally lead to a crossover in the mechanism responsible for the resistive switching, as we have shown. This implies that the presence of a MIT in large part determines whether electroforming will take place, and at which temperature it is possible. As a result, the device shows volatile (thermal) switching close to the transition, and nonvolatile filament formation at lower temperatures. These results might be of importance for the design of VO_x nanodevices in fields such as neuromorphic computing, where both volatile and nonvolatile resistive switching are required to mimic the behavior of neurons and synapses, respectively [10].

Once it takes place, electroforming completely changes the R vs T properties of the device. The details of the MIT reveal that it is composed of multiple closely spaced resistance jumps, indicating that several crystallites have formed in the filament with slightly different stoichiometry. Thus, the presence of compounds with well-defined stoichiometries restricts the variability in the electroformed resistive switches, giving a high degree of control.

The coupling of resistive switching and metal-insulator transitions achieved in our devices has immediate implications for fields like neuromorphic computing or memristive memories [7–10]. The presence of hysteresis loops in the $R(T)$ properties of the filament provides the device with an additional memory mechanism: the resistance will depend also on its thermal history. This thermal

dependence adds an extra control mechanism to the system, in addition to the well-known voltage control of traditional metal-oxide memristors, allowing alternative functionalities. One consequence of these effects is that the I - V characteristics of the filament are highly nonlinear, as shown in the inset of Fig. 1(c). This nonlinearity results in a threshold voltage around 0.1 V, below which it is hard to resolve whether the system is in the high or low resistance state, but above it both states are easily identified. Such a clear threshold for the readout voltage of a memristor would, for instance, solve the limiting and longstanding problem of sneak paths in resistive random access memories [34,35].

IV. CONCLUSIONS

In conclusion, we have studied the resistive switching in VO_2 and V_2O_3 nanodevices. We find a high temperature regime in which the thermal breakdown frustrates the electroforming of a conductive path. In contrast, at low temperatures it is possible to apply high-enough voltages to create a filament of different VO_x phases between the electrodes. Surprisingly, the $R(T)$ properties after the switching change drastically and several metal-insulator transitions appear in the device as a consequence of the formation of these phases in the gap. The vanadate family, with its large number of correlated oxides very close in stoichiometry, allows these effects to be observed. Moreover, oxygen migration has been shown to create ordered correlated oxide phases which exhibit electronic properties similar to their bulk or thin film counterparts. These results could inspire similar experiments in other oxide families which show different electronic orderings depending on the oxygen stoichiometry, such as, for instance, the MIT in nickelates and niobates or the different magnetic orderings in iron oxides.

ACKNOWLEDGMENTS

We thank M. J. Rozenberg for helpful discussions. The authors acknowledge support from the Vannevar Bush Faculty Fellowship program sponsored by the Basic Research Office of the Assistant Secretary of Defense for Research and Engineering and funded by the Office of Naval Research through Grant No. N00014-15-1-2848. J. d. V. and J. T. thank Fundación Ramón Areces for their funding. A. C. acknowledges financial support by the Alexander von Humboldt Foundation and the Gordon and Betty Moore Foundation.

[1] S. Tsui, A. Baikalov, J. Cmaidalka, Y. Y. Sun, Y. Q. Wang, Y. Y. Xue, C. W. Chu, L. Chen, and A. J. Jacobson, Field-induced resistive switching in metal-oxide interfaces, *Appl. Phys. Lett.* **85**, 317 (2004).

- [2] R. Waser and M. Aono, Nanoionics-based resistive switching memories, *Nat. Mater.* **6**, 833 (2007).
- [3] D. B. Strukov, G. S. Snider, D. R. Stewart, and R. S. Williams, The missing memristor found, *Nature (London)* **453**, 80 (2008).
- [4] J. J. Yang, M. D. Pickett, X. Li, D. A. A. Ohlberg, D. R. Stewart, and R. S. Williams, Memristive switching mechanism for metal/oxide/metal nanodevices, *Nat. Nanotechnol.* **3**, 429 (2008).
- [5] K. Fujiwara, T. Nemoto, M. J. Rozenberg, Y. Nakamura, and H. Takagi, Resistance switching and formation of a conductive bridge in metal/binary oxide/metal structure for memory devices, *Jpn. J. Appl. Phys.* **47**, 6266 (2008).
- [6] D. H. Kwon, K. M. Kim, J. H. Jang, J. M. Jeon, M. H. Lee, G. H. Kim, X. S. Li, G. S. Park, B. Lee, S. Han, M. Kim, and C. S. Hwang, Atomic structure of conducting nanofilaments in TiO_2 resistive switching memory, *Nat. Nanotechnol.* **5**, 148 (2010).
- [7] Y. Zhou and S. Ramanathan, Mott memory and neuromorphic devices, *IEEE Proc.* **103**, 1289 (2015).
- [8] J. J. Yang, D. B. Strukov, and D. R. Stewart, Memristive devices for computing, *Nat. Nanotechnol.* **8**, 13 (2013).
- [9] M. Prezioso, F. Merrikh-Bayat, B. D. Hoskins, G. C. Adam, K. K. Likharev, and D. B. Strukov, Training and operation of an integrated neuromorphic network based on metal oxide memristors, *Nature (London)* **521**, 61 (2015).
- [10] I. K. Schuller and R. Stevens, Neuromorphic computing: From materials to systems architecture, U.S. Department of Energy, <https://science.energy.gov> (2015).
- [11] U. Celano, L. Goux, R. Degraeve, A. Fantini, O. Richard, H. Bender, M. Jurczak, and W. Vandervorst, Imaging the three-dimensional conductive channel in filamentary-based oxide resistive switching memory, *Nano Lett.* **15**, 7970 (2015).
- [12] J. Yao, L. Zhong, D. Natelson, and J. M. Tour, *In situ* imaging of the conductive filament in a silicon oxide resistive switch, *Sci. Rep.* **2**, 242 (2012).
- [13] T. Driscoll, H.-T. Kim, B.-G. Chae, M. Di Ventra, and D. N. Basov, Phase-transition driven memristive system, *Appl. Phys. Lett.* **95**, 043503 (2009).
- [14] S. Guénon, S. Scharinger, S. Wang, J. G. Ramírez, D. Koelle, R. Kleiner, and I. K. Schuller, Electrical breakdown in a V_2O_3 device at the insulator to metal transition, *Europhys. Lett.* **101**, 57003 (2013).
- [15] A. Zimmers, L. Aigouy, M. Mortier, A. Sharoni, S. Wang, K. G. West, J. G. Ramirez, and I. K. Schuller, Role of Thermal Heating on the Voltage Induced Insulator-Metal Transition in VO_2 , *Phys. Rev. Lett.* **110**, 056601 (2013).
- [16] Jeehoon Kim, Changyun Ko, A. Frenzel, S. Ramanathan, and J. E. Hoffman, Nanoscale imaging and control of resistance switching in VO_2 at room temperature, *Appl. Phys. Lett.* **96**, 213106 (2010).
- [17] U. Schwingenschlogl and V. Eyert, The vanadium magnéli phases $\text{V}_n\text{O}_{2n-1}$, *Ann. Phys. (Berlin)* **13**, 475 (2004).
- [18] Z. Yang, C. Ko, and S. Ramanathan, Oxide electronics utilizing ultrafast metal-insulator transitions, *Annu. Rev. Mater. Res.* **41**, 337 (2011).
- [19] S. Lee, K. Hippalgaonkar, F. Yang, J. Hong, C. Ko, J. Suh, K. Liu, K. Wang, J. J. Urban, X. Zhang, C. Dames, S. A. Hartnoll, O. Delaire, and J. Wu, Anomalously low thermal

- conductivity in metallic vanadium dioxide, *Science* **355**, 371 (2017).
- [20] A. S. McLeod, E. van Heumen, J. G. Ramirez, S. Wang, T. Saerbeck, S. Guenon, M. Goldflam, L. Andereg, P. Kelly, A. Mueller, M. K. Liu, I. K. Schuller, and D. N. Basov, Nanotextured phase coexistence in the correlated insulator V_2O_3 , *Nat. Phys.* **13**, 80 (2017).
- [21] M. M. Qazilbash, M. Brehm, B.-G. Chae, P.-C. Ho, G. O. Andreev, B. J. Kim, S. J. Yun, A. V. Balatsky, M. B. Maple, F. Keilmann, H. T. Kim, and D. N. Basov, Mott transition in VO_2 revealed by infrared spectroscopy and nano-imaging, *Science* **318**, 1750 (2007).
- [22] I. Lo Vecchio, J. D. Denlinger, O. Krupin, B. J. Kim, P. A. Metcalf, S. Lupi, J. W. Allen, and A. Lanzara, Fermi Surface in Metallic V_2O_3 from Angle-Resolved Photoemission: Mid-level Filling of e_g^{π} Bands, *Phys. Rev. Lett.* **117**, 166401 (2016).
- [23] Y. Ding, C.-C. Chen, Q. Zeng, H.-S. Kim, M. J. Han, M. Balasubramanian, R. Gordon, F. Li, L. Bai, D. Popov, S. M. Heald, T. Gog, H.-K. Mao, and M. van Veenendaal, Novel High-Pressure Monoclinic Metallic Phase of V_2O_3 , *Phys. Rev. Lett.* **112**, 056401 (2014).
- [24] M. Liu, H. Y. Hwang, H. Tao, A. C. Strikwerda, K. Fan, G. R. Keiser, A. J. Sternbach, K. G. West, S. Kittiwatanakul, J. Lu, S. A. Wolf, F. G. Omenetto, X. Zhang, K. A. Nelson, and R. D. Averitt, Terahertz field-induced insulator-to-metal transition in vanadium dioxide metamaterial, *Nature (London)* **487**, 345 (2012).
- [25] R. Lopez, L. C. Feldman, and R. F. Haglund, Jr., Size-Dependent Optical Properties of VO_2 Nanoparticle Arrays, *Phys. Rev. Lett.* **93**, 177403 (2004).
- [26] See Supplemental Material at <http://link.aps.org/supplemental/10.1103/PhysRevApplied.8.054041> for the V_2O_3 case.
- [27] Y. Li, S. Long, Y. Liu, C. Hu, J. Teng, Q. Liu, H. Lv, J. Suñé, and M. Liu, Conductance quantization in resistive random access memory, *Nanoscale Res. Lett.* **10**, 420 (2015).
- [28] B. Xu and N. J. Tao, Measurement of single molecule resistance by repeated formation of molecular junctions, *Science* **301**, 1221 (2003).
- [29] M. Rodriguez-Vega, M. T. Simons, E. Radue, S. Kittiwatanakul, J. Lu, S. A. Wolf, R. A. Lukaszew, I. Novikova, and E. Rossi, Effect of inhomogeneities and substrate on the dynamics of the metal-insulator transition in VO_2 films, *Phys. Rev. B* **92**, 115420 (2015).
- [30] A. Camjayi, C. Acha, R. Weht, M. G. Rodríguez, B. Corraze, E. Janod, L. Cario, and M. J. Rozenberg, First Order Insulator-to-Metal Phase Transition in the Paramagnetic 3D System $GaTa_4Se_8$, *Phys. Rev. Lett.* **113**, 086404 (2014).
- [31] G. Mazza, A. Amaricci, M. Capone, and M. Fabrizio, Field-Driven Mott Gap Collapse and Resistive Switch in Correlated Insulators, *Phys. Rev. Lett.* **117**, 176401 (2016).
- [32] G.-H. Buh, I. Hwang, and B. H. Park, Time-dependent electroforming in NiO resistive switching devices, *Appl. Phys. Lett.* **95**, 142101 (2009).
- [33] J. Jeong, N. Aetukuri, T. Graf, T. D. Schladt, M. G. Samant, and S. P. Parkin, Suppression of metal-insulator transition in VO_2 by electric-field-induced oxygen vacancy formation, *Science* **339**, 1402 (2013); J. Jeong, N. B. Aetukuri, D. Passarello, S. D. Conradson, M. G. Samant, and S. P. Parkin, Giant reversible, facet-dependent, structural changes in a correlated electron insulator induced by ionic liquid gating, *Proc. Natl. Acad. Sci. U.S.A.* **112**, 1013 (2015).
- [34] J. J. Yang, M.-X. Zhang, M. D. Pickett, F. Miao, J. P. Strachan, W.-D. Li, W. Yi, D. A. A. Ohlberg, B. J. Choi, W. Wu, J. H. Nickel, G. Medeiros-Ribeiro, and R. S. Williams, Engineering non-linearity into memristors for passive crossbar applications, *Appl. Phys. Lett.* **100**, 113501 (2012).
- [35] M. A. Zidan, A. M. Eltawil, F. Kurdahi, H. A. H. Fahmi, and K. N. Salama, Memristor multiple readout: A closed form solution for sneak paths, *IEEE Trans. Nanotechnol.* **13**, 274 (2014).